International Journal of Environmental & Agriculture Research (IJOEAR)
ISSN: [2454-1850]
[Vol-12, Issue-10, October- 2026]
Website: www.ijoear.com
Journal DOI: 10.25125/agriculture-journal

Avipoxvirus outbreak in cutaneous lesions of the red-cowled cardinal (*Paroaria dominicana*) and red-crested cardinal (*Paroaria coronata*): detection by histopathology and transmission electron microscopy

Nataly Alves Melo[1*]; Ana M Cristina R P F Martins[2]; Mathias Fritzen Pedroso[3]; Marcia Helena Braga Catroxo[4]

Electron Microscopy Laboratory, Research and Development Center in Animal Health, Biological Institute, São Paulo, SP, Brazil Biological Institute, Avenida Conselheiro Rodrigues Alves, 1252, Vila Mariana, São Paulo, SP, Brazil
*Corresponding Author

Received:- 15 September 2026/ Revised:- 23 September 2026/ Accepted:- 05 October 2026/ Published: 31-10-2026
Copyright @ 2026 International Journal of Environmental and Agriculture Research
This is an Open-Access article distributed under the terms of the Creative Commons Attribution Non-Commercial License (https://creativecommons.org/licenses/by-nc/4.0) which permits unrestricted Non-commercial use, distribution, and reproduction in any medium, provided the original work is properly cited.

Abstract— *The red-cowled cardinal (Paroaria dominicana) and red-crested cardinal (Paroaria coronata) are birds of the family Emberizidae naturally found in northeastern and southern Brazil, respectively. These species are targeted by illegal trade because of their colorful plumage and are considered potential viral reservoirs owing to their migratory characteristics. Avian pox is a highly infectious disease caused by poxviruses of the family Poxviridae and genus Avipoxvirus that affects domestic and wild birds. Between January 2006 and September 2007, 72 birds, including 14 red-crested cardinals and 58 red-cowled cardinals, were referred after sudden death by CRAS-PET to the Electron Microscopy Laboratory of the Biological Institute of São Paulo for investigation of viral agents. At necropsy, small cutaneous nodular lesions were observed on the feet of one red-crested cardinal and ten red-cowled cardinals. Some birds had lesions characteristic of avian pox on the feet and/or beaks, consisting of whitish or yellowish nodules and desquamating crusts. Lesion fragments were processed for histopathology and transmission electron microscopy. Light microscopy revealed hyperkeratosis, epithelial hyperplasia, hydropic degeneration, and eosinophilic inclusions corresponding to Bollinger bodies in skin and/or mucosal cells. Negative staining identified numerous typical poxvirus particles in ten crust-suspension samples from red-cowled cardinals and one from a red-crested cardinal. Some particles were enveloped and brick-shaped, with irregularly arranged tubules on the outer membrane, and measured 280 × 260 nm. Ultrathin sections revealed type A intracytoplasmic inclusion bodies, or Bollinger bodies, containing mature or complete oval viral particles measuring 330 × 260 nm, with a biconcave nucleus or dumbbell-shaped internal core. Type B inclusion bodies, immature particles budding from dense amorphous filamentous material, developing particles with spikes on their outer surface, fibrillar inclusions, and deformed nuclei with densely condensed chromatin were also identified. Immunocytochemistry with colloidal gold labeled viral particles and antigenic sites in intracytoplasmic vacuoles and cellular debris. This is the first record of avian pox in the red-crested cardinal (Paroaria coronata) and the second in the red-cowled cardinal (Paroaria dominicana).*

Keywords— Paroaria coronata; Paroaria dominicana; poxvirus; transmission electron microscopy.

I. INTRODUCTION

The red-cowled cardinal (*Paroaria dominicana*) (LINNAEUS, 1758) and the red-crested cardinal (*Paroaria coronata*) (MULLER, 1776) belong to the order Passeriformes and genus *Paroaria*. The red-cowled cardinal, also known as cabeça-vermelha or cardeal-do-nordeste, is characteristic of the Caatinga and occurs mainly in northeastern Brazil, although it is also

found in southern Bahia and Minas Gerais. The red-crested cardinal occurs in Brazil, Uruguay, Paraguay, Bolivia, and Argentina (SICK, 2001).

Both species are frequently affected by the illegal wildlife trade. The red-cowled cardinal has been identified as one of the most commonly traded species in open-air markets in the Recife Metropolitan Region and as the bird most frequently seized in the Campina Grande region, Paraíba (MENEZES et al., 2003; PEREIRA & BRITO, 2005). Of 1,808 birds seized by the São Paulo Department of Parks and Green Areas, 148 were red-cowled cardinals (*P. dominicana*) (CAVALHEIRO et al., 2003). Red-crested and red-cowled cardinals are also among the species most commonly seized in the South and Central-West regions, while the red-cowled cardinal is among those most commonly seized in southeastern and northeastern Brazil (IBAMA, 2007).

Wild birds are considered potential viral reservoirs because their migratory behavior allows long-distance movements and dissemination of viruses of epidemiological importance. In addition, stressors such as capture, transport, confinement, and dietary or climatic changes may trigger viral processes, leading to sudden outbreaks and varied clinical manifestations (CUBAS & GODOY, 2004).

Diseases affecting avian skin have gained increasing importance because they can cause reduced egg production and growth, blindness, and, in some cases, death. Although natural avian poxvirus infection is better known in domestic poultry, it has also been reported in free-living birds (FENNER et al., 1992).

Avian pox is caused by viruses of the family Poxviridae and genus *Avipoxvirus*. Poxviruses have double-stranded DNA genomes 130–375 kbp in length and encode 150–300 proteins. Replication occurs in the cytoplasm of infected cells in regions known as viral factories, where immature and mature particles can be observed. Some mature particles acquire an envelope near the Golgi complex and are subsequently released from the cell, whereas nonenveloped particles are released by cell lysis (FAUQUET et al., 2005; FENNER et al., 1992).

Transmission may occur through the bites of hematophagous insects or contact with contaminated food, water, secretions, and fomites. The virus cannot penetrate intact skin and requires cuts or abrasions in the skin or mucosa to establish infection (CUBAS & GODOY, 2004). The disease may occur in cutaneous, diphtheritic, or mixed forms, depending on strain virulence, lesion distribution, and host susceptibility. The cutaneous form, also termed dry pox and probably the most common form, is characterized by nodular, proliferative, or crusted wart-like lesions, mainly in featherless areas such as the legs, feet, beak, and periocular region. Mild lesions are generally small and cause little debilitation; however, extensive lesions can impair vision, feeding, and breathing. Lesions in feathered areas, especially subtle ones, may also go unnoticed. In the diphtheritic form, or wet pox, proliferative plaques or membranes develop on the mucosa of the oral cavity and pharynx and sometimes the larynx and trachea, potentially causing respiratory difficulty, emaciation, and death. Cutaneous and diphtheritic lesions may occur simultaneously, constituting the mixed presentation (HOFSTAD et al., 1988; WILLIAMS et al., 2021).

Histologically, lesions may show epithelial hyperplasia and hypertrophy, hydropic degeneration, and eosinophilic intracytoplasmic inclusion bodies, known as Bollinger bodies, in skin or mucosal cells (GREENACRE, 2005).

In a study conducted at Tietê Ecological Park during an outbreak involving birds seized from illegal trade, Catroxo et al. (2009) reported avian pox in seven red-cowled cardinals (*Paroaria dominicana*), as well as other passerine species. All examined birds had lesions, and typical poxvirus particles were demonstrated by transmission electron microscopy using negative staining. Ultrathin skin sections revealed type A, type B, or Bollinger intracytoplasmic inclusions and fibrillar inclusions, complete and incomplete particles, and deformed nuclei with marginalized chromatin.

Transmission electron microscopy is particularly suitable for rapid identification of infectious agents. Negative staining reveals the morphology and dimensions of viral particles, assisting in their identification and classification. In addition to being rapid, it requires only a small sample and enables the detection of different viral particles in a single preparation (DOANE & ANDERSON, 1987; ALMEIDA, 1983; HAZELTON & GELDERBLOM, 2003).

Immunoelectron microscopy may be used when the number of viral particles in a sample is low, enabling identification through both morphology and the specific antigen–antibody reaction (KATZ & KLOHN, 1984). Colloidal gold immunolabeling

enables detection and localization of viral antigens in infected cells and assists in identifying strains and antigenic variants (KJELDSBERG, 1986; PATTERSON & OXFORD, 1986).

II. OBJECTIVE

To diagnose poxvirus infection in cutaneous lesions of the red-cowled cardinal (*Paroaria dominicana*) and red-crested cardinal (*Paroaria coronata*) using histopathology and transmission electron microscopy, including negative staining and colloidal gold immunolabeling.

III. MATERIALS AND METHODS

3.1 Description of the outbreak

Between January 2006 and September 2007, 72 birds from the Wildlife Recovery Center of Tietê Ecological Park, including 14 red-crested cardinals and 58 red-cowled cardinals, were referred after sudden death to the Electron Microscopy Laboratory of the Biological Institute, São Paulo, SP, Brazil.

3.2 Necropsy

The birds underwent necropsy. When lesions resembling avian pox were observed, they were collected and their location and extent recorded. One part of each lesion was fixed in 10% formalin and the other in 2.5% glutaraldehyde and refrigerated. Formalin-fixed samples were embedded in paraffin for light microscopy, whereas glutaraldehyde-fixed samples were embedded in Spurr resin for transmission electron microscopy.

3.2.1 Routine hematoxylin and eosin (H&E) histology

Organ fragments fixed in 10% buffered formalin were dehydrated, cleared, embedded in paraffin, and sectioned at 5 µm using a microtome. Following deparaffinization with xylene, sections were stained with hematoxylin and eosin, mounted with coverslips and Entellan, and examined using a conventional bright-field light microscope.

3.2.2 Negative-staining technique

This rapid diagnostic technique creates electron-dense contrast around the particle, causing electron beams encountering its surface to be deflected and producing a clear image of the particle's outer surface (BRENNER & HORNE, 1959).

Lesion fragments were suspended in 0.1 M phosphate buffer, pH 7.0. Drops of these suspensions were used to incubate metal grids coated with collodion film and carbon, which were subsequently negatively stained with 2% ammonium molybdate, pH 5.0 (BRENNER & HORNE, 1959; HAYAT & MILLER, 1990; MADELEY, 1997).

3.2.3 Resin embedding followed by positive staining

Lesion fragments were fixed in 2.5% glutaraldehyde in 0.1 M phosphate buffer, pH 7.0, postfixed in 1% osmium tetroxide in the same buffer, dehydrated through a graded acetone series from 50% to 100%, embedded in Spurr resin, and placed in an oven at 70°C for 36 hours for drying (GONZÁLEZ-SANTANDER, 1969). Ultrathin sections were cut using an ultramicrotome and positively stained with 2% uranyl acetate (WATSON, 1958) and 0.5% lead citrate (REYNOLDS, 1963).

3.2.4 Immunocytochemistry

3.2.4.1 Immunocytochemistry in negative staining

Copper grids previously coated with collodion film and carbon were incubated on 40-µL drops of viral suspension (antigen), exposed to specific antiserum diluted 1:80, and washed with PBS. They were then incubated with a secondary antibody (protein A conjugated to 10-nm colloidal gold particles) diluted 1:20 in 0.5% PBS and negatively stained with 2% ammonium molybdate, pH 5.0 (KNUTTON, 1995).

3.2.4.2 Post-embedding technique in ultrathin sections

After the fragments were embedded in Spurr resin, the blocks were sectioned and ultrathin sections collected on nickel grids. The grids were washed in BSA + Tween 20 in PBS, pH 7.0, incubated in 5 mM ammonium chloride (blocking and preventing specific antibody binding to free aldehyde groups in fixed cells), and washed in BSA + Tween 20 at pH 7.0. They were then incubated with primary antibody at 1:80 in 1% PBS/BSA for 4 hours, washed in BSA + Tween 20 in PBS, pH 7.0, incubated with secondary antibody (protein A–gold) at 1:10 in 1% PBS/BSA, washed in PBS, pH 7.0, and fixed with 2.5% glutaraldehyde

in distilled water. After washing, the grids were stained with uranyl acetate and lead citrate. At the beginning and end of processing, grids were treated with sodium metaperiodate (saturated solution) (KNUTTON, 1995; PADRÓN et al., 1998).

IV. RESULTS

4.1 Necropsy

Necropsies were performed at the Electron Microscopy Laboratory of the Biological Institute of São Paulo, São Paulo, Brazil. All 58 adult red-cowled cardinals (*Paroaria dominicana*) and 14 adult red-crested cardinals (*Paroaria coronata*), of both sexes, were necropsied and examined for the presence, location, and severity of lesions. Of these, 10 red-cowled cardinals (17.24%) and one red-crested cardinal (7.14%) exhibited lesions characteristic of avian poxvirus infection (Figs. 1 and 2).



FIGURE 1: Red-cowled cardinal (*Paroaria dominicana*) with a mild avian pox lesion on one foot (arrow)



FIGURE 2: Red-crested cardinal (*P. coronata*) with evident avian pox lesions on both feet (arrow)

4.2 Routine hematoxylin and eosin (H&E) histology

Light microscopy revealed hyperkeratosis and epithelial hyperplasia with eosinophilic inclusions (Bollinger bodies) in skin and/or mucosal cells and hydropic degeneration, consistent with avipoxvirus infection.

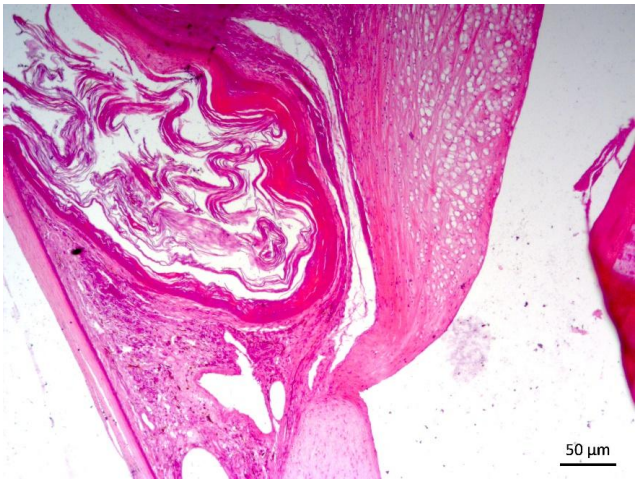


FIGURE 3: Photomicrograph showing thickening of the epidermis, marked hyperkeratosis, and vacuolated epithelial cells (hyperkeratotic proliferative dermatitis with epithelial changes consistent with cutaneous avian pox). ×100 (H&E)

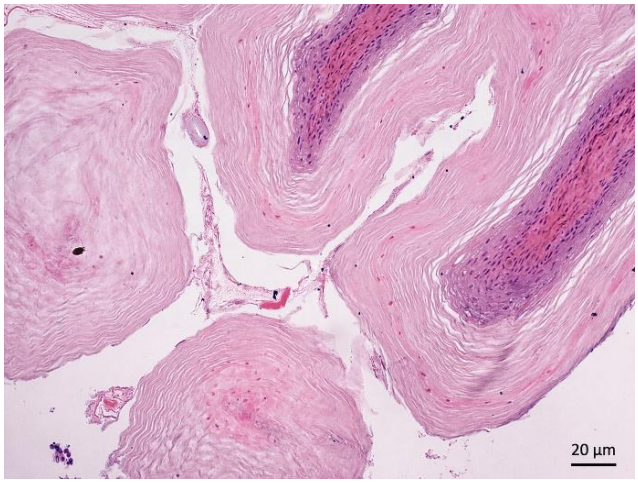


FIGURE 4: Photomicrograph showing epidermal thickening with marked lamellar hyperkeratosis. Areas of epithelial cell vacuolation are present. ×200 (H&E)

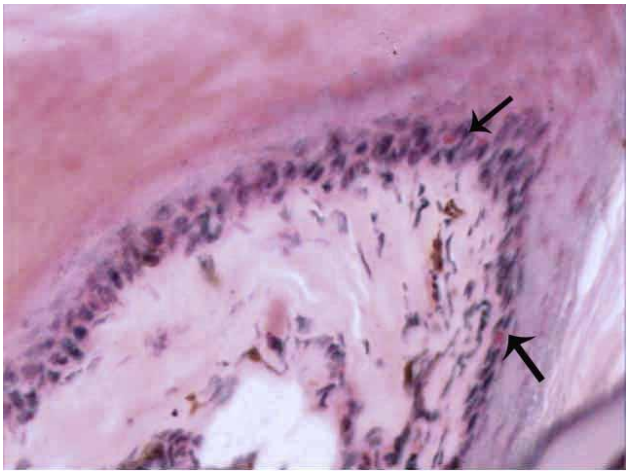


FIGURE 5: Photomicrograph showing thickening of the epidermis and marked lamellar hyperkeratosis, with areas of epithelial cell vacuolation and intracytoplasmic inclusion bodies in epithelial cells (arrow). ×400 (H&E)

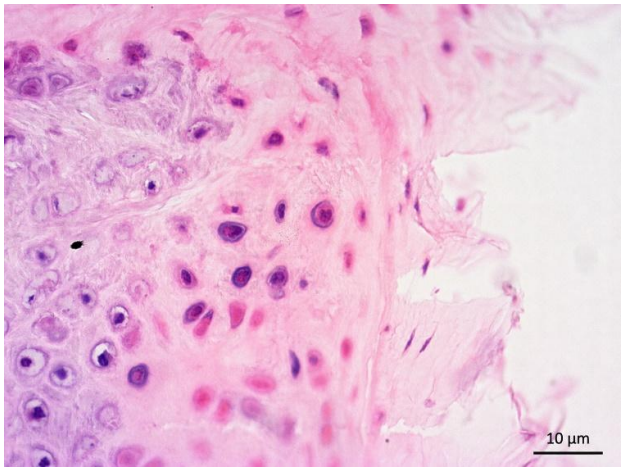


FIGURE 6: Photomicrograph showing epithelial cells with ballooning degeneration (black arrow) and eosinophilic intracytoplasmic inclusion bodies (orange arrow), associated with epidermal hyperplasia and marked hyperkeratosis. ×620 (H&E)

4.3 Transmission electron microscopy

4.3.1 Negative staining (rapid preparation) technique

Transmission electron microscopy using the negative staining technique revealed a large number of typical poxvirus particles in skin lesions or crusts from 10 samples of red-cowled cardinals (*Paroaria dominicana*) and one sample of a red-crested cardinal (*Paroaria coronata*) (Figs. 7 and 8). The particles were ovoid in shape, with an irregular arrangement of tubules on their outer surface; some were enveloped. They measured, on average, 280 nm in length × 260 nm in diameter.

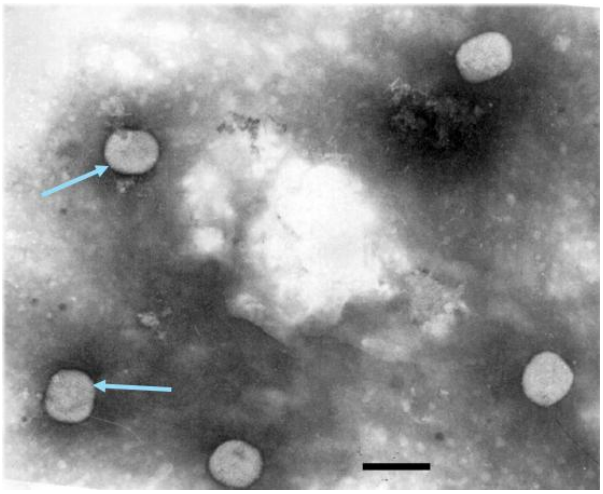


FIGURE 7: Poxvirus-like particles in a lesion from a red-crested cardinal (*P. coronata*), visualized by negative staining (arrow). Scale bar: 420 nm

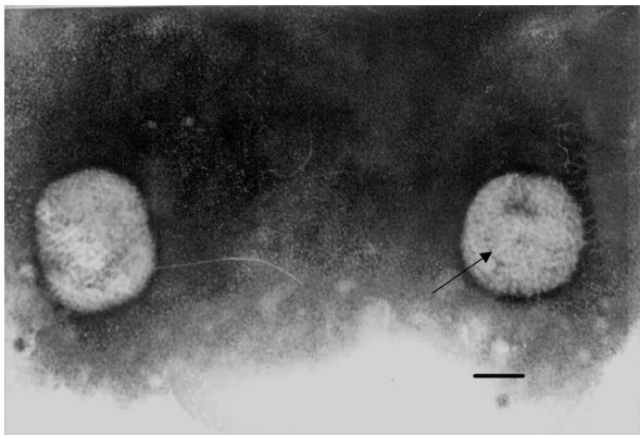


FIGURE 8: Poxvirus-like particles from a lesion in a red-crested cardinal (*P. coronata*), with microtubules distributed over the outer membrane (arrow). Scale bar: 230 nm

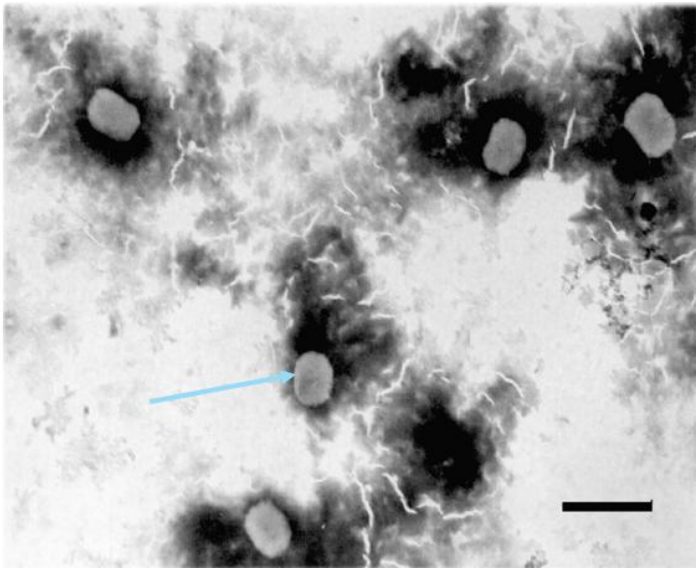


FIGURE 9: Poxvirus-like particles (arrow) from a cutaneous foot lesion of a red-cowled cardinal (*P. dominicana*). Scale bar: 320 nm.

4.3.2 Resin embedding technique

In the ultrathin sections examined, three distinct types of intracytoplasmic inclusion bodies were identified. Type A, or Bollinger bodies (Fig. 10, red arrow), were membrane-bound structures containing a large number of mature viral particles (Fig. 10). The particles measured approximately 200 × 300 nm and exhibited the characteristic dumbbell-shaped internal core flanked by two lateral bodies (Fig. 10, yellow arrow) and surrounded by an external envelope (Fig. 10, blue arrow).

Type B inclusion bodies were electron-dense and contained viral particles budding from a dense, amorphous matrix (Figs. 11, 12, red arrow) and acquiring an envelope (yellow arrow). Viral particles in formation, exhibiting spikes on their outer surface (red arrow), were also observed budding from the amorphous inclusion (yellow arrow) (Fig. 13). In addition, fibrillar inclusions composed of groups of fibrils or lamellar structures (Fig. 14, arrow) were observed. These structures occurred in groups ranging from two to five elements and occasionally exhibited transverse striations.

The nuclei were deformed and exhibited peripheral chromatin margination (Fig. 15, arrow).

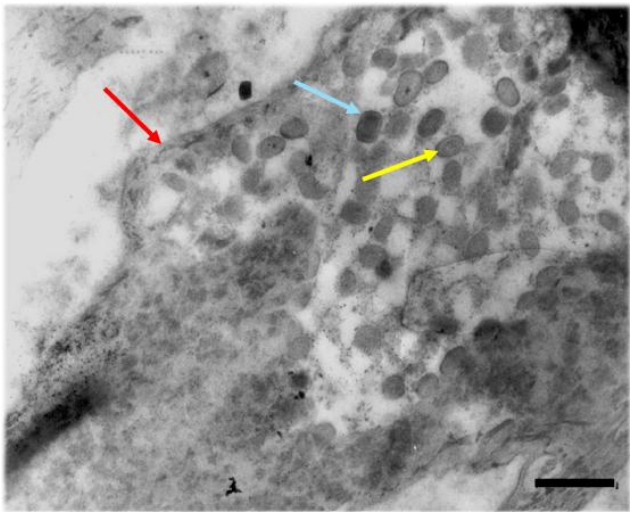


FIGURE 10: Intracytoplasmic inclusion bodies—Bollinger bodies (red arrow). Enveloped particles (blue arrow). Note the figure-eight-shaped lateral bodies in some non-enveloped particles (yellow arrow). Scale bar: 960 nm

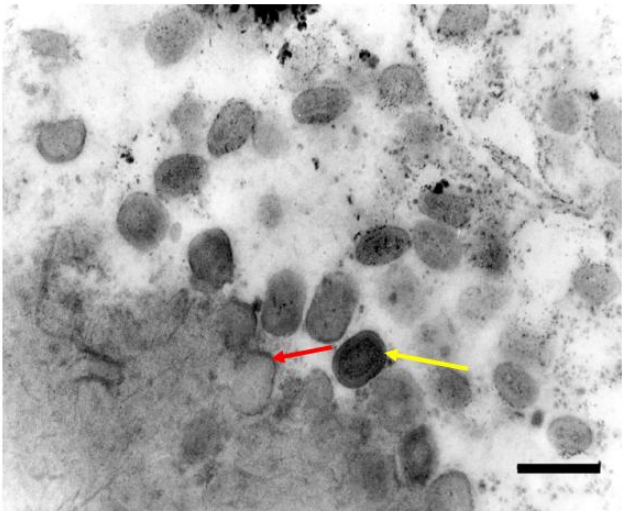


FIGURE 11: Type B electron-dense inclusion, containing viral particles budding from a dense, amorphous matrix (red arrow) and another acquiring an envelope (yellow arrow). Scale bar: 270 nm

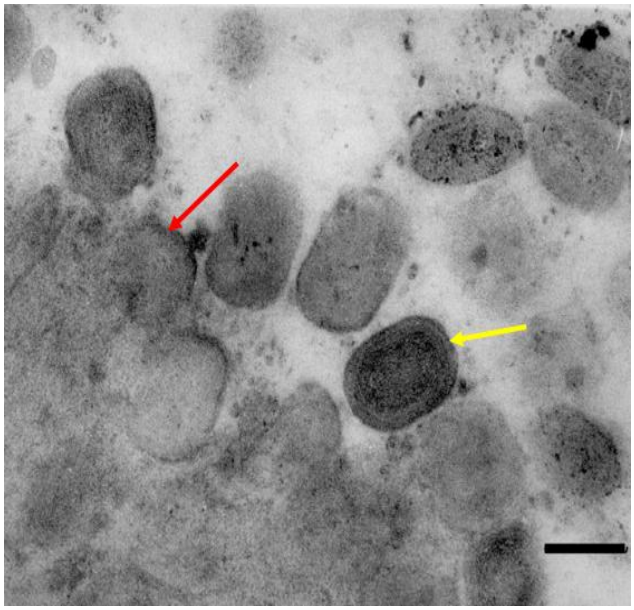


FIGURE 12: Enlargement of Figure 11. Enveloped poxvirus particles (yellow arrow) and budding particles (red arrow). Scale bar: 260 nm

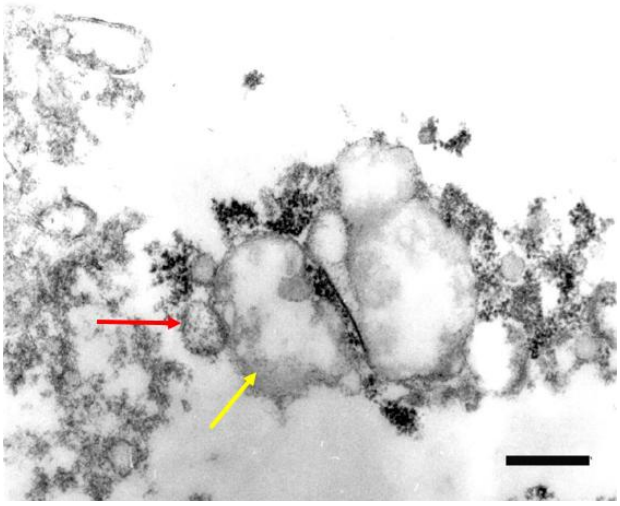


FIGURE 13: Viral particles in formation, showing spikes on the outer surface (red arrow), budding from an amorphous inclusion (yellow arrow). Scale bar: 440 nm

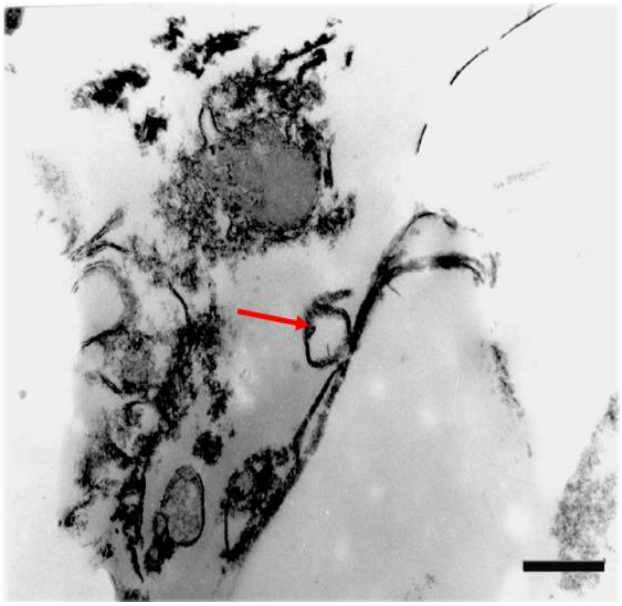


FIGURE 14: Intracellular fibrillar inclusions consisting of groups of fibrils, probably associated with the initial stage of virion formation (arrow). Scale bar: 360 nm

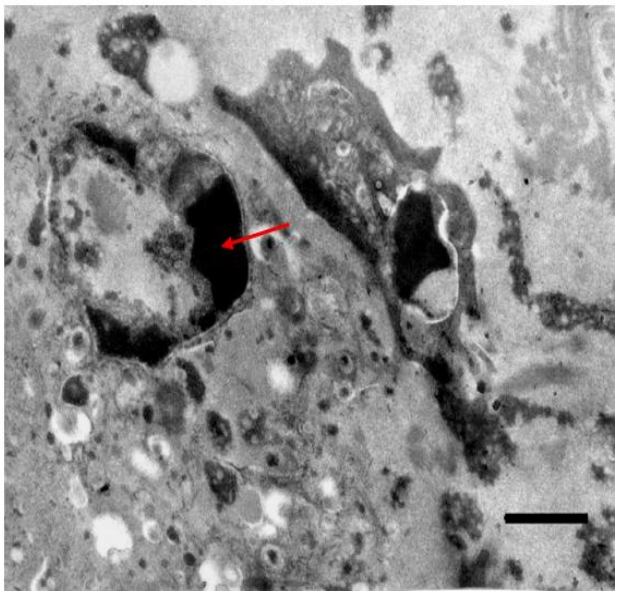


FIGURE 15: Cell from a lesion of a red-cowled cardinal (*P. dominicana*) showing an amorphous nucleus with condensed chromatin (arrow). Scale bar: 940 nm

4.3.3 Immunocytochemistry

4.3.3.1 Immunocytochemistry by negative staining technique

In the immunocytochemistry technique, the antigen–antibody reaction was highlighted by colloidal gold particles, demonstrating a positive reaction between the poxvirus particle and its specific antibody (Figs. 16 and 17).

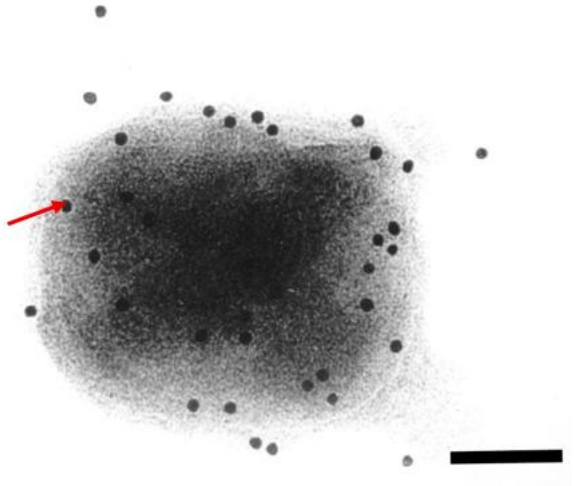


FIGURE 16: Poxvirus particle from a cutaneous lesion of a red-cowled cardinal (*P. dominicana*), labeled with gold microspheres. Scale bar: 100 nm

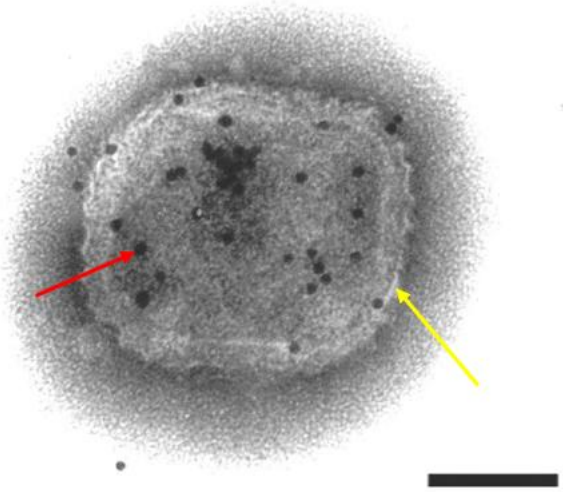


FIGURE 17: Poxvirus particle from a cutaneous lesion of a red-crested cardinal (*P. coronata*), labeled with gold microspheres (red arrow). Note the external envelope (yellow arrow). Scale bar: 120 nm

4.3.3.2 Immunocytochemistry post-embedding technique

Examination by transmission electron microscopy of ultrathin sections subjected to this technique revealed colloidal gold particles labeling viral antigenic sites within intracytoplasmic vacuoles (red arrow) and associated with cellular debris scattered throughout the cytoplasm (yellow arrow) (Fig. 18).

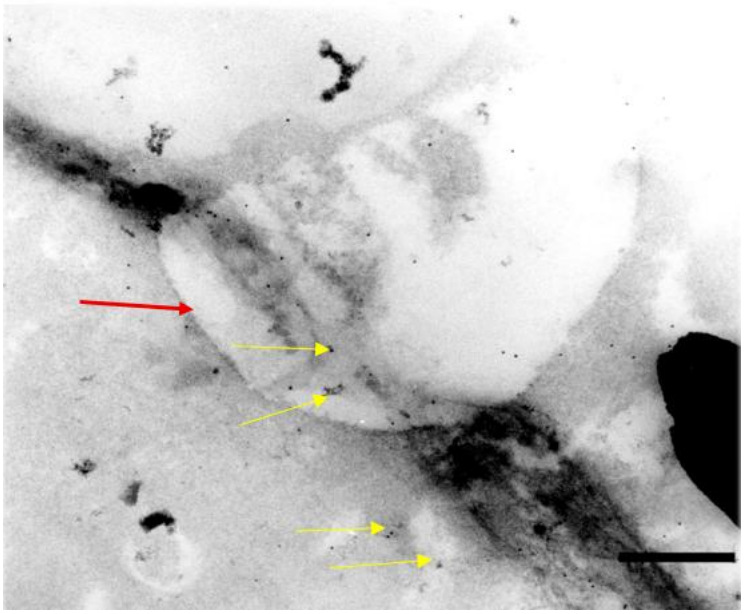


FIGURE 18: Vacuole (red arrow) in a lesion cell from a red-cowled cardinal. Antigenic sites within the vacuole were labeled by gold particles (yellow arrow) during immunocytochemistry. Scale bar: 440 nm.

V. DISCUSSION

This study investigated poxvirus in cutaneous lesions of 58 red-cowled cardinals (*Paroaria dominicana*) and 14 red-crested cardinals (*Paroaria coronata*) referred to the Electron Microscopy Laboratory between January 2006 and September 2007. Proliferative, nodular, and crusted lesions confined to the feet were observed in 10 red-cowled cardinals (17.24%) and one red-crested cardinal (7.14%). The identification of particles with typical poxvirus morphology by negative staining, their demonstration in ultrathin sections, and colloidal gold immunolabeling, interpreted alongside the histopathological changes, confirmed infection in the samples examined.

The observed frequencies were close to those described by DOCHERTY et al. (1985), who found 17% positivity in *Carpodacus mexicanus*, and WINGATE (1980), who reported 7.4% in *Phaethon lepturus*. However, these percentages should not be regarded as prevalence estimates for natural populations of *P. dominicana* and *P. coronata*, because the birds examined came from a recovery center and had experienced specific conditions of seizure, transport, crowding, and stress. The considerable variation among species and studies may be related to host species, region, environmental conditions, the type of population examined, and the diversity of avipoxvirus lineages (WILLIAMS; TRUCHADO; BENÍTEZ, 2021; GYURANECZ et al., 2013; SARKER; ATHUKORALA; RAIDAL, 2021).

All positive birds had the cutaneous form of avian pox. The location of lesions on the feet is consistent with the predilection of avipoxviruses for featherless regions more exposed to minor abrasions or insect bites. CATROXO et al. (2009, 2012, 2022a, b) also described nodular and crusted lesions on the feet of wild passerines during outbreaks in São Paulo. Although lesions may involve the periocular regions, beak, cere, head, limbs, and oral cavity, no lesions consistent with the diphtheritic form or mixed infection were observed in this study.

Histopathologically, lesions showed marked epidermal hyperplasia, acanthosis, and ballooning degeneration of keratinocytes, associated with eosinophilic intracytoplasmic inclusions consistent with Bollinger bodies. Hyperplasia and acanthosis account for the enlargement and nodular appearance of the lesions, while ballooning degeneration demonstrates progressive epithelial cell damage. Similar changes, including epithelial hyperplasia, vacuolar degeneration, necrosis, and Bollinger bodies, have been described in domestic, wild, and captive birds infected with avipoxvirus (MOHAMED et al., 2024; COLOM-RIVERO et al., 2025; SÁ et al., 2025).

Histopathology revealed lesion distribution and the tissue response to infection, but electron microscopy was decisive in directly demonstrating viral particles and the different stages of their morphogenesis. Negative staining of suspensions of crusts and lesion fragments revealed numerous typical poxvirus particles. The virions were brick-shaped, showed irregularly arranged tubules on the outer membrane, and measured an average of 280 × 260 nm; some particles were enveloped. This combination of size, shape, and surface organization is characteristic of the family Poxviridae and was also observed in avian samples by CATROXO et al. (2009, 2012, 2022a, b), TERREGINO et al. (1999), and WELI et al. (2003).

Negative staining proved particularly useful as a rapid direct visualization method, because it allowed viral morphology to be recognized in lesion suspensions without prior isolation. Its performance, however, depends on the number of particles in the sample and the quality of preparation. Failure to visualize virions by this technique would not exclude infection, as shown by METZ et al. (1985), who did not detect particles in cloacal lesion fragments from turkeys. Conversely, KRONE et al. (2004) detected particles in skin and tongue lesions of a peregrine falcon by negative staining despite unsuccessful viral isolation in cell culture or embryonated eggs. It is important to emphasize that successful application of negative staining relies on mechanically and thermally stable support films reinforced with a thin carbon layer and mounted on metal grids before sample application. This preparation provides greater structural stability during processing and examination, minimizing artifacts and facilitating preservation and clear visualization of viral particles by transmission electron microscopy (GENTILE & GELDERBLOM, 2014).

In ultrathin sections of skin and crusts, transmission electron microscopy revealed membrane-bound type A intracytoplasmic inclusion bodies, or Bollinger bodies, containing large numbers of mature or complete particles. Virions were oval, measured an average of 330 × 260 nm, and had characteristic internal organization, with a biconcave dumbbell-shaped core and lateral bodies. These ultrastructural features are consistent with the architecture of mature poxvirus particles and have been described in different cases of avian pox (THIELE et al., 1979; COX, 1980; WINGATE, 1980; McDONALD et al., 1981; FITZNER et al., 1985; NUTTALL et al., 1985; REED; SCHRADER, 1989; KREUDER et al., 1999; KIM et al., 2003; SMITS et al., 2005; BEYTUT; HALIGÜR, 2007; CATROXO et al., 2009, 2012).

Type B intracytoplasmic inclusions, consisting of dense, amorphous filamentous material from which immature viral forms emerged, were also identified. Developing particles were observed acquiring an outer envelope, whereas others showed progressively more defined organization until reaching the configuration of mature virions (CATROXO et al., 2009, 2012). The coexistence of immature, intermediate, and mature forms in the same tissue provides morphological evidence of active replication and allows successive stages of viral morphogenesis to be followed. This finding is consistent with the poxvirus replication cycle taking place in specialized cytoplasmic areas, often called viral factories, formed by granular electron-dense material separated from cellular membranes (MOSS, 2007).

The correlation between histopathology and electron microscopy strengthened the interpretation of the results. On light microscopy, Bollinger bodies appeared as eosinophilic inclusions in the cytoplasm of enlarged, degenerated keratinocytes. In ultrathin sections, corresponding regions contained viral particles at different stages of development, from immature structures associated with fibrillar and electron-dense material to mature particles with defined internal organization. Thus, histopathology demonstrated the extent of the tissue's proliferative and cytopathic response, while electron microscopy confirmed the viral nature of the intracytoplasmic structures and revealed their subcellular organization.

Fibrillar inclusions consisting of groups of two to four cross-striated fibrils located between virions were also observed. Similar structures have been described in other studies of avian pox in *Paroaria dominicana*, *Sporophila caerulescens*, and *Sporophila albogularis* (Catroxo et al., 2009), in *Gnorimopsar chopi* (Catroxo et al., 2012), and in studies of swinepox by TEPPEMA and BOER (1985) and BERSANO et al. (2003). In the present material, their spatial association with developing particles suggests a relationship with early sites of viral assembly or with the reorganization of cellular components during infection. Because the precise nature of these fibrils was not determined by a specific technique, this interpretation must remain cautious; morphology alone cannot establish whether they are a viral component or a specific cytoskeletal structure.

Nuclear changes, including nuclear deformation and densely condensed or marginalized chromatin, were also identified (CATROXO et al., 2009, 2012). Although conspicuous, they do not indicate intranuclear replication, because poxviruses synthesize and assemble their particles in the cytoplasm (BERSANO et al., 2003). These changes should be interpreted as consequences of cellular degeneration and the extensive cytoplasmic reorganization caused by infection. The concurrent presence of ballooning degeneration on light microscopy, nonspecific nuclear changes, and cytoplasmic viral factories in ultrathin sections demonstrates the progression of cellular injury in affected areas.

Immunocytochemistry combined with electron microscopy added specificity to morphological identification. With negative staining, colloidal gold particles intensely labeled the virions, demonstrating the antigen–antibody reaction. In ultrathin sections, labeling was also observed at antigenic sites within intracytoplasmic vacuoles and in cellular debris dispersed throughout the cytoplasm. Thus, immunolabeling not only supported identification of the observed particles (CATROXO et al., 2009, 2012, 2022a, b) but also localized viral antigens in cellular structures associated with infection, a method used by VANSLYKE & HRUBY (1994) and HELJASVAARA et al. (2001) to localize vaccinia virus proteins.

Immunoelectron microscopy is particularly useful when morphology allows identification of a viral family but confirmation of the antigenic nature of the particles or localization of viral components within tissue is desired. Agreement among virion shape and size, their location within inclusion bodies, the different maturation stages, and colloidal gold labeling strengthened the diagnosis. The technique had previously been used to demonstrate poxvirus in avian pox crusts from *Paroaria dominicana*, *Sporophila caerulescens*, *Sporophila albogularis*, *Gnorimopsar chopi*, *Tersina viridis*, and canaries (CATROXO et al., 2009, 2012, 2022a, b), as well as in swinepox lesions (BERSANO et al., 2003), confirming its value in combining morphology and immunological specificity.

Together, the three electron microscopy approaches provided complementary information. Negative staining enabled rapid detection of large numbers of particles and assessment of their external morphology; ultrathin sections demonstrated their intracytoplasmic location, the organization of inclusion bodies, and the sequence of virion maturation; and colloidal gold immunolabeling confirmed the antigenic nature of the observed structures. This integration is the principal strength of the study, extending beyond simple visualization of isolated particles to document the relationship among tissue lesions, cytoplasmic replication, and virion formation.

The recorded clinical findings, including anorexia, weight loss, difficulty moving, diarrhea, dehydration, and death, may have been exacerbated by the location of lesions on the feet and by the conditions in which the birds reached the recovery center. These clinical signs have also been observed in other birds, including parrots (McDONALD et al., 1981; GERLACH et al., 1998), *Platycercus* sp. and *Psephotus haematonotus* (MURER et al., 2018), red-cowled cardinals, brejais, and coleirinhos (CATROXO et al., 2009), blackbirds (CATROXO et al., 2012), canaries, and swallow tanagers (CATROXO et al., 2022a, b). Extensive foot lesions interfere with perching, movement, and access to food. Large nodules may obstruct vision or the opening of the beak, interfering with the bird's ability to eat and drink and potentially causing mortality (MURER et al., 2018). In birds from illegal trade, factors such as stress, overcrowding, and coinfections may trigger disease. Other clinical signs, including blindness, blepharitis, conjunctivitis, rhinitis, depression, dyspnea, lethargy, hypothermia, and pneumonia, have also been described (McDONALD et al., 1981; BOOSINGER et al., 1982; NUTTALL et al., 1985; RAIDAL et al., 1996; KREUDER

et al., 1999; KRONE et al., 2004; MEDINA et al., 2004; GREENACRE, 2005; GULBAHAR, 2005; MURER et al., 2018). Neurological signs may occasionally be observed in parrots (GREENACRE, 2005).

The frequent presence of mosquitoes during the warmer months at Tietê Ecological Park may have contributed to the development of the outbreak. Avipoxviruses may be mechanically transmitted by hematophagous insects or through contact with crusts, secretions, contaminated surfaces, or breaks in the skin (GERLACH, 1984; GUSTAFSON et al., 1997). GUSTAFSON et al. (1997) associated an avian pox outbreak in a chicken flock with fleas attached to the lesions. Introducing infected birds into susceptible groups poses an additional risk, underscoring the importance of quarantine, separating birds with lesions, environmental sanitation, and vector control (RITCHIE et al., 1994).

This study documents avian pox in *P. coronata* and *P. dominicana*; its main contribution is the integrated demonstration of infection at different levels of observation. Histopathology characterized the proliferative and degenerative epithelial response, while electron microscopy provided the central evidence for confirmation: it revealed the external morphology of the particles, demonstrated their location and maturation within inclusion bodies, and confirmed the presence of viral antigens through colloidal gold immunolabeling.

Studies of this important disease should continue to expand knowledge of its occurrence, epidemiology, and distribution and to inform prevention and control methods. These actions are essential for protecting both free-living birds and species threatened with extinction, contributing to their conservation. In addition, disease monitoring and control are important to reduce the risk of transmission to birds kept in breeding facilities and commercial poultry operations, minimizing outbreaks and consequent potential production and economic losses.

VI. CONCLUSION

This is the first record of avian pox in the red-crested cardinal (*Paroaria coronata*) and the second in the red-cowled cardinal (*Paroaria dominicana*). The combination of histopathological findings, visualization of viral particles by negative staining and in ultrathin sections, and colloidal gold immunolabeling confirmed the presence of poxvirus and demonstrated different stages of its morphogenesis in cutaneous lesions.

The results show that wild birds are also susceptible to infectious diseases capable of impairing mobility, feeding, and overall condition. This finding is particularly important for wildlife conservation, because diseases such as avian pox may increase the vulnerability of wild populations, including species threatened with extinction, especially when associated with animal trafficking, crowding, stress, inadequate husbandry, and the presence of vectors. Accordingly, early diagnosis, quarantine, isolation of affected birds, biosafety measures, and insect control are essential in wildlife screening and recovery centers.

ACKNOWLEDGEMENTS

The authors thank the Wildlife Recovery Center of Tietê Ecological Park (CRAS-PET) for providing the bird samples and the Electron Microscopy Laboratory of the Biological Institute of São Paulo for technical support.

CONFLICT OF INTEREST

The authors declare that there is no conflict of interest.

REFERENCES

[1] Almeida, J. D. (1983). Uses and abuses of diagnostic electron microscopy. *Current Topics in Microbiology and Immunology*, *104*, 147-158.

[2] Bersano, J. G., Catroxo, M. H. B., Villalobos, E. M. C., Leme, M. C. M., Martins, A. M. C. P. F., Peixoto, Z. M. P., Portugal, M. A. S. C., Monteiro, R. M., Ogata, R. A., & Curi, N. A. (2003). Varíola suína: Estudo sobre a ocorrência de surtos nos estados de São Paulo e Tocantins, Brasil. *Arquivos do Instituto Biológico*, *70*(3), 269-278.

[3] Beytut, E., & Haligür, M. (2007). Pathological, immunohistochemical, and electron microscopic findings in respiratory tract and skin of chickens naturally infected with avipoxvirus. *Turkish Journal of Veterinary and Animal Sciences*, *31*(5), 311-317.

[4] Boosinger, T. R., Winterfield, R. W., Feldman, D. S., & Dhillon, A. S. (1982). Psittacine pox virus: Virus isolation and identification, transmission and cross-challenge studies in parrots and chickens. *Avian Diseases*, *26*(2), 437-444.

[5] Brenner, S., & Horne, R. W. (1959). A negative staining method for high resolution electron microscopy of viruses. *Biochimica et Biophysica Acta*, *34*, 103-110.

[6] Catroxo, M. H. B., Pongiluppi, T., Melo, N. A., Milanelo, L., Petrella, S., Martins, A. M. C. R. P. F., & Rebouças, M. M. (2009). Identification of poxvirus under transmission electron microscopy during outbreak period in wild birds, in São Paulo, Brazil. *International Journal of Morphology*, *27*(2), 577-585.

[7] Catroxo, M. H. B., Martins, A. M. C. R. P. F., Petrella, S., & Milanelo, L. (2012). Detection of poxvirus using transmission electron microscopy techniques during outbreak in Bay-Winged Cowbird (*Gnorimopsar chopi*). In C. C. Perez-Marin (Ed.), *A bird's-eye view of veterinary medicine* (Chapter 25, pp. 557-566). InTechOpen.

[8] Catroxo, M. H. B., Martins, A. M. C. R. P. F., Milanelo, L., Fitorra, L. S., Petri, B. S. S., & Santos, E. M. (2022a). Detection of avipoxvirus in a cutaneous lesion of a swallow tanager (*Tersina viridis*) by transmission electron microscopy. *Brazilian Journal of Animal and Environmental Research*, *5*(1), 1311-1320.

[9] Catroxo, M. H. B., Milanelo, L., Martins, A. M. C. R. P. F., & Cassiano, L. (2022b). Occurrence of avian pox outbreaks in wild and canary commercial breedings: Diagnosis through electron transmission microscopy and histopathology techniques. *International Journal of Environmental & Agriculture Research*, *8*(6), 18-26.

[10] Cavalheiro, S. K., Narvaes, L. V. P., Marcondes, P. N., & Fantinato, F. M. (2003). Animais silvestres: Tráfico em São Paulo–Brasil. *Arquivos do Instituto Biológico*, *70*(Suppl. 3).

[11] Colom-Rivero, A. F., Ponce, L. M., Ramirez, D. P., Caballero-Hernandez, L., Rivero-Harrera, C., Santana, C. M. S., & Sierra, E. (2025). Pathological and molecular characterization of Avipoxvirus infection in *Burhinus oedicnemus* in the Canary Islands. *Veterinary Sciences*, *12*(9), Article 849.

[12] Cox, W. R. (1980). Avian pox infection in a Canada goose (*Branta canadensis*). *Journal of Wildlife Diseases*, *16*(4), 623-626.

[13] Cubas, Z. S., & Godoy, S. N. (2004). *Algumas doenças de aves ornamentais*. www.adma.com.br

[14] Doane, F. W., & Anderson, M. (1987). Electron microscopy in diagnostic virology. *Journal of Virological Methods*, *56*, 652-653.

[15] Docherty, D. E., & Long, R. I. R. (1985). Isolation of poxvirus from a house finch, *Carpodacus mexicanus* (Muller). *Journal of Wildlife Diseases*, *22*(3), 420-422.

[16] Fauquet, C. M., Mayo, A. M., Maniloff, J., Desselberger, U., & Ball, L. A. (2005). *Virus taxonomy: Classification and nomenclature of viruses* (8th ed.). Elsevier Academic Press.

[17] Fenner, F., Bachmann, P. A., Gibbs, E. P. J., Murphy, F. A., Studdert, M. J., & White, D. O. (1992). *Virologia veterinaria*. Acribia.

[18] Fitzner, R. E., Miller, R. A., Pierce, C. A., & Rowe, S. E. (1985). Avian pox in red-tailed hawk (*Buteo jamaicensis*). *Journal of Wildlife Diseases*, *21*(3), 298-301.

[19] Gentile, M., & Gelderblom, H. R. (2014). Electron microscopy in rapid viral diagnosis: An update. *New Microbiologica*, *37*, 403-422.

[20] Gerlach, H. (1984). Virus diseases in pet birds. *Veterinary Clinics of North America: Small Animal Practice*, *14*(2), 299-316.

[21] González-Santander, R. (1969). *Técnicas de microscopia electrónica en biología*. Aguilar.

[22] Greenacre, C. B. (2005). Viral diseases of companion birds. *Veterinary Clinics of North America: Exotic Animal Practice*, *8*(1), 85-105.

[23] Gulbahar, M. Y., Çabalar, M., & Boynukara, B. (2005). Avipoxvirus infection in quails. *Turkish Journal of Veterinary and Animal Sciences*, *29*, 449-454.

[24] Gustafson, C. R., Bickford, A. A., Cooper, G. L., & Charlton, B. R. (1997). Sticktight fleas associated with fowl pox in a backyard chicken flock in California. *Avian Diseases*, *41*, 1006-1009.

[25] Gyuranecz, M., Foster, J. T., Dán, Á., Ip, H. S., Egstad, K. F., Parker, P. G., Higashiguchi, J. M., Skinner, M. A., Hogle, U., Kreizinger, Z., Dorrestein, G. M., Solt, S., Sós, E., Kim, Y. J., Uhart, M., Pereda, A., González-Hein, G., Hidalgo, H., Blanco, J., & Erdélyi, K. (2013). Worldwide phylogenetic relationship of avian poxviruses. *Journal of Virology*, *87*(9), 4938-4951.

[26] Hayat, M. A., & Miller, S. E. (1990). *Negative staining*. McGraw-Hill Publishing Company.

[27] Hazelton, P. R., & Gelderblom, H. R. (2003). Electron microscopy for rapid diagnosis of emerging infectious agents in emergent situations. *Emerging Infectious Diseases*, *9*(3), 294-303.

[28] He, L., Zhang, Y., Jia, Y., Li, Z., Shang, K., Ding, K., Yu, H., & Sarker, S. (2023). A novel pathogenic avipoxvirus infecting oriental turtle dove (*Streptopelia orientalis*) in China shows a high genomic and evolutionary proximity with the pigeon avipoxviruses isolated globally. *Microbiology Spectrum*, *11*(5), e0119323.

[29] Heljasvaara, R., Rodríguez, D., Risco, C., Carrascosa, J. L., Esteban, M., & Rodríguez, J. R. (2001). The major core protein P4a (A10L gene) of vaccinia virus is essential for correct assembly of viral DNA into the nucleoprotein complex to form immature viral particles. *Journal of Virology*, *75*(13), 5778-5795.

[30] Hofstad, M. S., Barnes, H. J., Calnek, B. W., Reid, W. M., & Yoder, H. W. (1988). *Diseases of poultry* (8th ed.). Iowa State University Press.

[31] IBAMA. (n.d.). *Instituto Brasileiro do Meio Ambiente e dos Recursos Naturais Renováveis. Fauna–tráfico de animais silvestres*. www.ibama.gov.br

[32] Katz, D., & Kohn, A. (1984). Immunosorbent electron microscopy for detection of viruses. *Advances in Virus Research*, *29*, 169-194.

[33] Kim, T. J., Schnitzlein, W. M., McAloose, D., Pessier, A. P., & Tripathy, D. N. (2003). Characterization of an avianpox virus isolated from an Andean condor (*Vultur gryphus*). *Veterinary Microbiology*, *96*(3), 237-246.

[34] Kjeldsberg, E. (1986). Use of gold IgG complexes and human antisera for electron microscopy identification of hepatitis A virus and polioviruses. *Journal of Virological Methods*, *13*, 207.

[35] Knutton, S. (1995). Electron microscopical methods in adhesion. *Methods in Enzymology*, *253*, 145-158.

[36] Kreuder, C., Irizarry-Rovira, A. R., Janovitz, E. B., Deitschel, P. J., & De Nicola, D. B. (1999). Avian pox in sanderlings from Florida. *Journal of Wildlife Diseases*, *35*(3), 582-585.

[37] Krone, O., Essbauer, S., Wibbelt, G., Isa, G., Rudolph, M., & Gough, R. E. (2004). Avipoxvirus infection in peregrine falcons (*Falco peregrinus*) from a reintroduction programme in Germany. *Veterinary Record*, *154*(4), 110-113.

[38] Madeley, C. R. (1997). Origins of electron microscopy and virus diagnosis. *Journal of Clinical Pathology*, *50*(6), 454-456.

[39] McDonald, S. E., Lowenstine, L. J., & Ardams, A. A. (1981). Avian pox in blue-fronted Amazon parrots. *Journal of the American Veterinary Medical Association*, *179*(11), 1218-1222.

[40] Medina, F. M., Ramírez, G. A., & Hernández, A. (2004). Avian pox in white-tailed laurel-pigeons from the Canary Islands. *Journal of Wildlife Diseases*, *40*(2), 351-355.

[41] Menezes, I. R., Albuquerque, H. N., & Medeiros, F. P. (2003). Inventário de aves traficadas na cidade de Campina Grande. In *Congresso Brasileiro de Ornitologia* (Vol. 11, p. 26). Feira de Santana, BA, Brasil.

[42] Metz, A. L., Hatcher, L., Newman, A. J., & Halvorson, D. A. (1985). Venereal pox in breeder turkeys in Minnesota. *Avian Diseases*, *29*(3), 850-853.

[43] Mohamed, R. I., Elsamadony, H. A., Alghamdi, R. A., Eldin, A. L. A. Z., El-Shemy, A. M., Bahshwan, S. M. A., El-Saadony, M. T., El-Sayed, H. S., El Tarabily, K. A., & Saad, A. S. A. (2024). Molecular and pathological screening of the current circulation of fowlpox and pigeon pox virus in backyard birds. *Poultry Science*, *103*(12), 104249.

[44] Moss, B. (2007). Poxviridae: The viruses and their replication. In *Virology* (5th ed., pp. 2905-2975). Lippincott Williams & Wilkins.

[45] Murer, L., Westenhofen, M., Kommers, G. D., Furian, T. Q., Borges, K. A., Kunert-Filho, H. C., Streck, A. F., & Lovato, M. (2018). Identification and phylogenetic analysis of clade C Avipoxvirus in a fowlpox outbreak in exotic psittacines in southern Brazil. *Journal of Veterinary Diagnostic Investigation*, *30*(6), 946-950.

[46] Nuttall, P. A., Brooke, M. D., & Perrins, C. M. (1985). Poxvirus infection of the Manx shearwater (*Puffinus puffinus*). *Journal of Wildlife Diseases*, *21*(2), 120-124.

[47] Padrón, T. S. (1998). Técnicas de imunocitoquímica. In *Técnicas básicas de microscopia eletrônica aplicada às ciências biológicas.* Rio de Janeiro.

[48] Patterson, S., & Oxford, J. S. A. (1986). Analysis of antigenic determinants on internal and external proteins of influenza virus and identification of antigenic subpopulations of virions in recent field isolates using monoclonal antibodies and immunogold labelling. *Archives of Virology*, *88*, 189.

[49] Pereira, G. A., & Brito, M. T. (2005). Diversidade de aves silvestres brasileiras comercializadas nas feiras livres da Região Metropolitana de Recife, Pernambuco, Brasil. *Atualidades Ornitológicas*, (126), 14.

[50] Pereira, W. L. A., Gabriel, A. L. M., Monger, S. G. B., Moraes, L. A., Queiroz, D. K. S., & Souza, A. J. S. (2014). Cutaneous tumor-like lesions associated with infection by avipoxvirus in a *Dendrocygna autumnalis*. *Ciência Animal Brasileira*, *15*(2), 234-238.

[51] Raidal, S. R., Gill, J. H., & Cross, G. M. (1996). Pox in ostrich chicks. *Australian Veterinary Journal*, *73*(1), 32-33.

[52] Reed, W. M., & Schrader, D. L. (1989). Pathogenicity and immunogenicity of mynah pox virus in chickens and bobwhite quail. *Poultry Science*, *68*(5), 631-638.

[53] Reynolds, E. S. (1963). The use of lead citrate at high pH as an electron-opaque stain in electron microscopy. *Journal of Cell Biology*, *17*, 208-212.

[54] Ritchie, B. W., Harrison, G. J., & Harrison, L. R. (1994). *Avian medicine: Principles and application* (pp. 865-874). Wingers Publishing Inc.

[55] Sá, J. J. S., Aranda, V. M. P. T., Withoeft, J. A., Marian, L., Baron, A., Cristo, T., & Casagrande, R. A. (2025). Avipoxvirus outbreak in captive Psittaciformes in southern Brazil. *Pesquisa Veterinária Brasileira*, *45*, E07635.

[56] Sarker, S., Athukorala, A., & Raidal, S. R. (2021). Molecular characterization of a novel pathogenic avipoxvirus from an Australian passerine bird, mudlark (*Grallina cyanoleuca*). *Virology*, *554*, 66-74.

[57] Sick, H. (2001). *Ornitologia brasileira*. Nova Fronteira.

[58] Smits, J. E., Tella, J. L., Carrete, M., Serrano, D., & López, G. (2005). An epizootic of avian pox in endemic short-toed larks (*Calandrella rufescens*) and Berthelot's pipits (*Anthus berthelotii*) in the Canary Islands, Spain. *Veterinary Pathology*, *42*, 59-65.

[59] Teppema, J. S., & de Boer, G. F. (1975). Ultrastructural aspects of experimental swinepox with special reference to inclusion bodies. *Archives of Virology*, *49*, 151-163.

[60] Terregino, C., Catelli, E., Delogu, M., Capua, I., & Tonelli, A. (1999). Poxvirus infection in a blue bonnet parrot. *Veterinary Record*, *145*(9), 264.

[61] Thiele, J., Kiel, H., & Adolphs, H. D. (1979). Avian pox: An ultrastructural study on a cherrug falcon. Brief report. *Archives of Virology*, *62*(1), 77-82.

[62] Vanslyke, J. K., & Hruby, D. E. (1994). Immunolocalization of vaccinia virus structural proteins during virion formation. *Virology*, *198*, 624-635.

[63] Watson, M. L. (1958). Staining of tissue sections for electron microscopy with heavy metals. *Journal of Biophysical and Biochemical Cytology*, *4*, 475-478.

[64] Weli, S. C., & Tryland, M. (2011). Avipoxviruses: Infection biology and their use as vaccine vectors. *Virology Journal*, *8*(49), 1-15.

[65] Williams, R. A. J., Truchado, D. A., & Benítez, L. A. (2021). Review on the prevalence of poxvirus disease in free-living and captive wild birds. *Microbiology Research*, *12*(2), 403-418.

[66] Wingate, D. B., Barker, I. K., & King, N. W. (1980). Poxvirus infection of the white-tailed tropicbird (*Phaethon lepturus*) in Bermuda. *Journal of Wildlife Diseases*, *16*(4), 619-622.